

Impact of controlled extensional flow during extrusion of PP, PVDF and LDPE

Marcel Andrey de Goes¹ , João Paulo Ferreira Santos²  and Benjamim de Melo Carvalho^{1*} 

¹*Departamento de Engenharia de Materiais, Universidade Estadual de Ponta Grossa – UEPG, Ponta Grossa, PR, Brasil*

²*Departamento de Engenharia de Materiais, Centro Federal de Educação Tecnológica de Minas Gerais, Belo Horizonte, MG, Brasil*

*benjamim@uepg.br

Abstract

The structure and properties of semi-crystalline polymers can be drastically tailored by extensional flows. In this work, polypropylene (PP), Polyvinylidene fluoride (PVDF) and Low Density Polyethylene (LDPE) were melt extruded through a sequence of rings designed to apply controlled extensional flows in the polymer melts. The effects of extensional flow on the structure and properties of the extruded filaments were then evaluated by mechanical tensile tests, dynamic-mechanical analysis (DMA) and Differential Scanning Calorimetry (DSC). The DMA and tensile tests revealed a significant increase in terms of static and dynamic moduli for the polymers extruded through the extensional flow device. PP, PVDF and LDPE had their dynamic moduli enhanced 19%, 40% and 77%, respectively. These results were ascribed to the enhancement in crystallinity and orientation degree of the polymer chains induced by the extensional flow. The crystallinity was increased around 9% for PP, PVDF and LDPE extruded under extensional conditions.

Keywords: *extensional flow, extrusion, semi-crystalline polymers, crystallinity increase.*

How to cite: Goes, M. A., Santos, J. P. F., & Carvalho, B. M. (2022). Impact of controlled extensional flow during extrusion of PP, PVDF and LDPE. *Polímeros: Ciência e Tecnologia*, 32(2), e2022019. <https://doi.org/10.1590/0104-1428.20210085>

1. Introduction

The extensional flow is a type of pressure flow in which the speed of material undergoes increases or decreases in the flow direction. This type of flow occurs in many thermoplastics processing methods, such as extrusion, film blowing and fiber spinning^[1]. Although it is relatively common in the polymer industry, the study of effects of extensional flow on properties of polymer materials is not so trivial. Several studies have been dedicated to evaluating the effects of dispersion enhancement provided by extensional flow when applied to nanocomposite processing through the construction of laboratory-scale devices^[2-5]. A more recent approach in this field seeks to evaluate components to enhance the extensional flow in twin-extrusion processing, which provides gains in dispersive power in the production of immiscible blends^[6,7], for example. In a previous work of our group^[8] an extensional flow device was employed during single-screw extrusion to enhance the degree of dispersion of montmorillonite nanoclay (MMT) and multiwalled carbon nanotubes (MWCNT) through the melted PVDF. The improvement in terms of dispersive mixing was demonstrated by reductions in mean cluster sizes of 44% and 55%, respectively, for the MWCNT and MMT. However, the effect of extensional flow on the structure and properties of the polymer matrix was not studied.

It is known that over 50% of industrially applied polymers in the world are semi-crystalline. Among these, polyolefins are the most representative class, with Polypropylene (PP) and Polyethylene (PE) standing out^[9]. PP is a thermoplastic polymer that has characteristics such as low density, low cost, chemical resistance and can be processed by several methods^[10,11]. LDPE is a semi-semi-crystalline polymer that has an opaque appearance, tensile strength, rigidity and chemical resistance, flexibility even at a low temperatures^[12]. Poly (vinylidene fluoride) (PVDF) is a semi-crystalline polymer that presents piezoelectric properties that make it attractive for applications such as energy conversion applications involving microelectric-mechanical devices, electromechanical actuators and energy harvesters^[13,14].

Due to the commercial importance of semi-crystalline polymers, over the decades studies have been dedicated to understanding their kinetics and the influence on other properties and much progress has been made since the works of the pioneers Boon et al.^[15,16] and Agar et al.^[17]. Processing conditions like pressure^[18,19], cooling rate^[20,21], and flow conditions^[22,23] may cause impacts on the crystallinity of the polymeric material and can cause changes in the kinetics, final microstructure or crystallinity content. The application of fluxes during or after the crystallization of the melt polymer can result in molecular orientation, that is, alignment

of chains which in turn brings significant changes in the crystallization process^[24]. This phenomenon is known as “Flow-Induced Crystallization” (FIC) and can significantly reduce the induction time for crystallization^[25], increase the number of nucleation points for crystals to originate and also provide gains in terms of mechanical properties^[1].

The crystallinity can be increased by the use of extensional flows that can be applied during crystallization of the polymer melt and produce molecular orientation, which can dramatically affect the crystallization process. In the work’s of Chellamuthu et al.^[24] and Bischoff White et al.^[26], an extensional filament stretching rheometer was used with a custom-built oven to investigate the effect of uniaxial flow on the crystallization of isotactic poly-1-butene and isotactic polypropylene, respectively. The authors demonstrated that it is possible to increase crystallinity up to 25% with the controlled use of stretching rates during crystallization. In the work of Chellamuthu et al.^[24], this increase in crystallinity was associated with the increasing orientation and alignment of the polymer chains in extensional flows, which enhances the thread-like precursors responsible for the formation of the crystals in the *shish-kebab* morphology. However, *shish-kebab* morphology is not always formed in crystallization by introducing an extensional rate, as pointed out in the study of Bischoff White et al.^[26].

Processing methods for thermoplastics typically involves the application of heat and stress, thus inducing the plastic to assume the desired shape^[25]. The flow type used during the processing can significantly change the final properties of the products^[27,28]. In this context, in the current work, we studied the impact of increase the extensional flow during the extrusion process on the thermal and mechanical properties of semi-crystalline polymers. Although the effects are known, their quantification is not something so easily found in the literature. Three polymers were selected for this work: Polypropylene (PP), Polyvinylidene fluoride (PVDF) and Low Density Polyethylene (LDPE), three of

the most common semi-crystalline thermoplastics employed in the current industry.

2. Materials and Methods

2.1 Materials

Polypropylene (PP), H301, was acquired from Braskem. According to the manufacturer, the density and melt flow index (MFI) were 0.905 g/cm³ and 10 g/10 min (at 230 °C/2.16 kgf), respectively. The PVDF, Kynar 1000HD, was purchased from Arkema Inc, density and melt flow index (MFI) were 1.78 g/cm³ and 1.1 g/10 min (at 230 °C/5.0 kgf), respectively. Low Density Polyethylene (LDPE) also acquired from Braskem, SPB681, presents a density of 0.922 g/cm³ and MFI of 3.8 g/10 min (at 190 °C/2.16 kgf).

2.2 Processing of semi-crystalline polymers with and without extensional Flow

Sample preparation was carried out in a single screw mini-extruder (Filmaq3d STD) with a die of 4 mm in diameter for filament production. For processing with the aid of the extensional flow, a device was used in place of the die, which consists of a series of 7 rings alternating their internal diameters between 2 and 4 mm. The die acted as “eighth ring”, with a diameter equal to 4 mm, a schematic of this device is shown in Figure 1. The use of the total number of 8 rings is based on the work of Jamali et al.^[29], where it was proven that this number of rings is sufficient to promote the most significant effects of the application of extensional flow in the processing of nanocomposites. The extruded filaments were collected using a filament winder that has a water-cooling system. To determine the extensional deformation rate ($\dot{\epsilon}$) provided with the use of the extensional flow device, we used Equation 1 presented in the work of Feigl et al.^[30]:

$$\dot{\epsilon}' = \frac{Q}{\pi R_0^2 L} (e^{\epsilon_H} - 1) \quad (1)$$

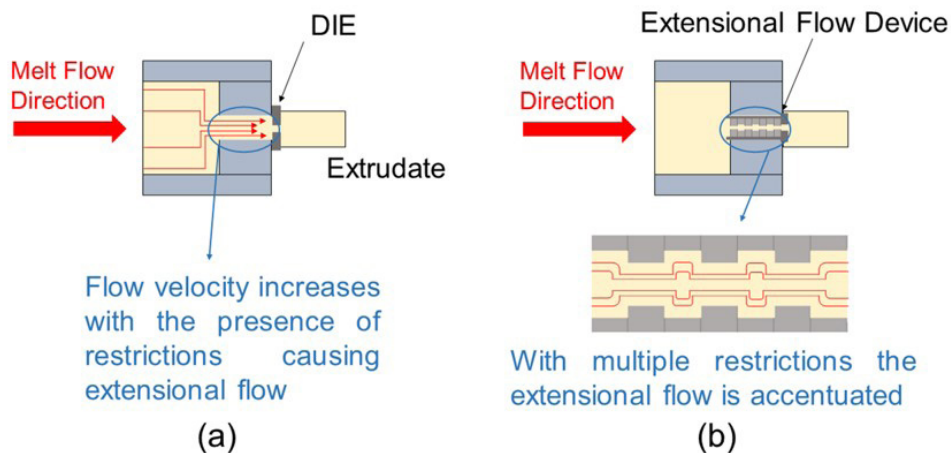


Figure 1. Schematic representation of processing without (a) and with (b) the extensional flow device.

ϵ_H refers to the true strain known as logarithmic or Hencky strain and we can determine it by the equation:

$$\epsilon_H = \ln \left(\frac{R_0^2}{R_c^2} \right) \quad (2)$$

Q is the flow rate which, considering the constant axial speed (v_z) is given by:

$$Q = 2\pi \int_0^R v_z \cdot r \cdot dz = \pi v_z R_0^2 \quad (3)$$

The value of v_z was considered to be the minimum tangential speed for the filament winder which was kept constant and was used in this estimate due to the water cooling system (approx. 25°C) forcing the filament to pass under the water after leaving the matrix, preventing the winding system from contributing with a significant stretch rate. R_o and R_e correspond, respectively, to the largest and smallest internal radius in the extensional flow channel; L is the length of the rings. With the values for the constructed extensional flow device, we find an extensional strain rate of 33.19 s⁻¹. To ensure this elongation rate for all processed polymers, temperature adjustment was performed, according to Table 1, in order to provide the same flow rate (Q), providing the same value of $\dot{\epsilon}$, since the other parameters are geometry dependent.

The samples were processed by extrusion without the extensional flow device and with this device. For each polymer, two separate extrusions were performed the first in a conventional manner and the second using the extensional flow device. Samples processed with the aid of extensional flow will present the suffix “-el”. All materials were processed in neat form.

PVDF was dried in an oven (70 °C) for 24 hours before extrusion. The other semi-crystalline polymers did not go through this process. Subsequently, about 25 g of material was used to formulate each sample. The formulations were prepared twice each, aiming to carry out two processes for each, the first in a conventional manner and the second using the extensional flow device. The processing temperature was used as shown in Table 1 and screw rotation was 30 rpm for all samples.

2.3 Characterization of Filaments

The filaments were evaluated mechanically at room temperature (25°C) using a universal testing machine (Shimadzu Autograph AGS - 10 kN) without an extensometer. Ten samples were tested for each one of the six compositions shown in Table 1 with a length of 100 mm being that the

spacing between claws used was 50 mm, a tensile strain rate of 5 mm/min and a maximum deformation (ϵ) value of 0.21 mm/mm. The maximum tensile strength (σ_{max}) was measured by the equipment and Young Moduli (E) for the crystalline polymers were determined by the tangent method (ASTM D638).

Using the Discovery Hybrid Rheometer (DH-2) equipment from TA Instruments, measurements were made with the Linear Dynamic Mechanical Analysis (DMA) accessory for films and filaments. Filaments with a length of 50 mm were used with spacing between the claws of 35 mm. With the equipment operating in traction the system was adjusted to an axial load of 1 N, dynamic force at 30% of the axial load, frequency of 1 Hz, axial displacement 20 μ m and a temperature of 30°C. In this analysis, the storage moduli (E') and loss moduli (E'') were measured. The analysis was performed for two samples of each composition shown in Table 1, with eight measurements collected in each test.

Thermal properties of the samples were evaluated by differential scanning calorimetry (DSC). DSC was performed using an equipment from Shimadzu, DSC60. Two heating cycles were carried from 25 °C up to 200°C (PP and LDPE) and from 25°C to 220 °C (PVDF). The heating and cooling rates were 10 °C/min for PP LDPE and 20 °C/min for PVDF. All measurements were carried out under nitrogen (N_2) atmosphere using flow rate of 50 ml/min were used. The melting temperature (T_m) was determined according to the methodology of the standard ASTM D3418-15. The crystallinity was estimated from the heat of fusion, and using the value for 100% crystallinity of PP (138 J/g^[31]), PVDF (105 J/g^[32]) and LDPE (288 J/g^[33]).

3. Results and Discussions

3.1 Mechanical characterization

Figure 2 shows stress strain curves obtained from mechanical tensile tests. Table 2 summarizes the Maximum tensile strength (σ_{max}) and Young Moduli (E). It can be seen that there is a significant difference caused by the presence of the extensional flow on the mechanical tensile properties. When extruded under extensional flow, the stress strain curves exhibited an increase in stiffness of the polymers reflected in the slope of the curve in the region of elastic deformation. Münsterdt^[34] and Tabatabaei et al.^[35] demonstrated that extensional rates increase can result in an increase in the mechanical properties for semi-semi-crystalline polymers in the flow direction, this effect being dependent on process parameters such as cooling rate and stretching. This type of effect is usually associated as a result of the ability of the extensional flow to stretch and align the macromolecules in the direction of the flow^[36], or it may also be associated with the Flow-Induced Crystallization (FIC)^[24-26].

In addition to the behavior displayed on the elastic moduli, there was also an increase in maximum tensile strength (σ_{max}) values found for processing with extensional flow device. The increases were 18.51, 28.90, and 7.85% for PP-el, PVDF-el and LDPE-el, respectively. Such an increase can be an interesting effect to be applied in the production of filaments with improved mechanical properties.

Table 1. Processing conditions.

Compositions	Presence of Extensional Flow Device	Temperature (°C)
PP		200
PP-el	x	200
PVDF		270
PVDF-el	x	270
LDPE		200
LDPE-el	x	200

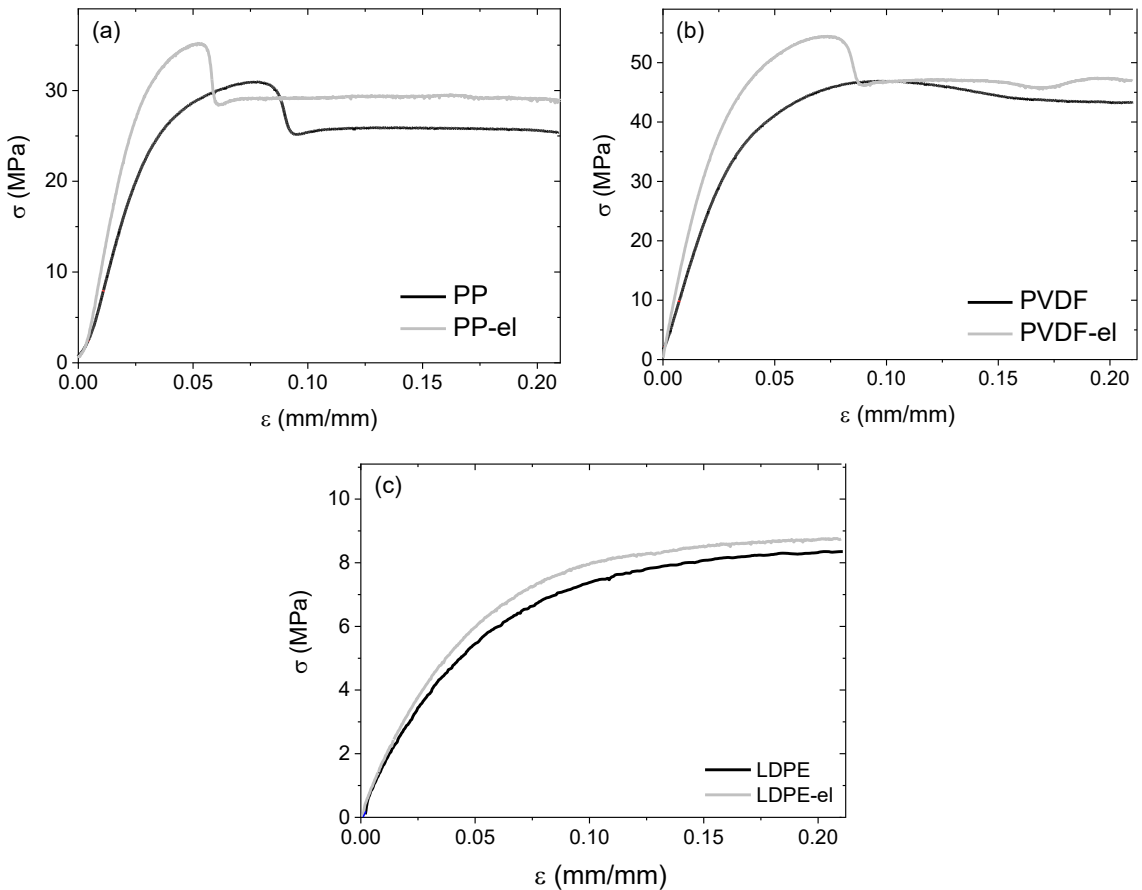


Figure 2. Stress (σ) versus strain (ϵ) curves for: (a) PP; (b) PVDF and (c) LDPE.

Table 2. Maximum tensile strength (σ_{\max}) and Young Moduli (E) for the semi-crystalline polymers.

Compositions	σ_{\max} (MPa)	Standard deviation	E (GPa)	Standard deviation
PP	29.99	1.50	0.77	0.017
PP-el	35.54	2.58	1.08	0.043
PVDF	46.30	1.50	1.32	0.014
PVDF-el	59.68	4.94	1.94	0.030
LDPE	9.30	0.40	0.14	0.005
LDPE-el	10.03	0.31	0.17	0.002

Dynamic mechanical analysis is an indispensable tool when evaluating the viscoelastic properties of semi-crystalline polymers^[37]. The properties measured by DMA for polymers processed with and without extensional flow are summarized in Table 3.

Young's modulus is typically associated with the storage modulus (E'), or also called the dynamic modulus, this property is commonly associated with the stiffness of the evaluated material^[38,39]. Based on this and the behavior displayed in tensile curves (Figure 2), we can say that the semi-crystalline polymers evaluated in this work showed greater stiffness when processed using the extensional flow device in the extrusion processing, according to the values presented in Table 3 and Figure 3. The observed increases in E' were 18.9%, 40.4%, 77.5%, respectively, for PP-el,

PVDF-el, and LDPE-el. Such results corroborate with the measures made in mechanical tensile tests that also pointed out an increase due to the accentuated extensional flow in the extrusion process. Regarding the differences between the E value (Table 2) and the E' (Table 3) values, they are possibly related to the lack of use of extensometer in the tensile test and to the loss of grip of the filaments during this analysis, which must have affected the measurements of deformation. The values obtained in this analysis for E' , the PP in the study of Das and Satapathy^[40] reports a similar value around 1.5 GPa also using extrusion processing. For the PVDF and LDPE, studies were found that indicate values around 3 GPa^[41,42] and 1 GPa^[43,44], respectively.

The loss modulus (E'') or also called dynamic loss modulus is usually associated with the viscous response of

the material and is related to its tendency to dissipate energy that has been applied to it^[38,39]. Concerning this property, the measured values (Table 3) demonstrate that the extensional flow contributes to its increase by 18.2%, 37.5% and 77.8% for PP-el, PVDF-el and LDPE-el, respectively. The dynamic loss moduli are often associated with “internal friction” and is a property sensitive to morphological changes and structural heterogeneities^[39,42]. From this perspective, we can interpret that the presence of the extensional flow resulted in some morphological change in the way the chains are organized, increasing the “internal friction” or, otherwise, increase the viscous response of the material associated with the values of E'' . This modification can be associated with the changes in the crystallinity of the polymers that may have been provided by the FIC phenomenon.

The complex moduli (E^*) also increase for semi-crystalline polymers processed with the extensional flow. The value of E^* can be visualized as the hypotenuse of a right triangle where its sides are the values of E' and E'' ^[39] thus the increase in the values of these components, due to

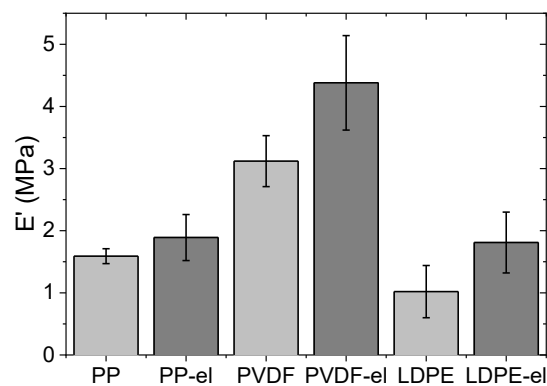


Figure 3. Storage moduli (E') measured at 1Hz and 30°C for the crystalline polymers.

the presence of elongational flow, also reflects an increase in the values of E^* . The increase in the calculated values of E^* were 18.9%, 42.6%, and 76.9% for PP-el, PVDF-el, and LDPE-el, respectively.

3.2 Differential Scanning Calorimetry – DSC

Figure 4 exhibits DSC curves of first fusion peak to semi-crystalline polymers and the main thermal properties are summarized in Table 4. For PP, a peak was observed around ≈ 166 °C, which is in line with values already available in other studies^[10,45,46] for α phase crystals. For PP-el, it is possible to notice a very smooth lateral shoulder at a temperature around 160 °C that may be associated with another phase induced by extensional flow, but this was not considered in our analysis, which may cause a slight variation in the measured values of crystallinity. The melting temperature (T_m) of PVDF and LDPE were, respectively, ≈ 170 °C and ≈ 112 °C which was ascribed to the melting of α phase crystals^[47] in PVDF and for LDPE the value is in agreement with the range of values in other works^[48,49]. Therefore, as shown in Table 4, no significant difference, at the melting temperature, was observed due to the presence of extensional flow device in processing, as shown in Table 4.

Table 4 shows an increase in crystallinity of polymers processed with the extensional flow device. The crystallinity increases were 9.1%, 8.5% and 9.3% respectively for PP-el, PVDF-el and LDPE-el. An increase in crystallinity reflects on the stiffness of the polymeric material^[50], which can partially justifies the effect on the values of E' (Table 3). It can also be related to the increase in the maximum tensile strength (σ_{max}) for the crystalline polymers (Table 2). It is worthy of note that in the second heating cycle performed in the DSC, the crystallinities (Table 4) of the samples processed with and without the extensional flow device are the same, showing differences of less than 1.3%. Another indication that this increase in crystallinity is associated with the processing history with the extensional flow device.

Table 3. Storage Modulus (E'), Loss Modulus (E'') and Complex Modulus (E^*) at 1Hz and 30°C for the semi-crystalline polymers.

Compositions	E' (GPa)	Standard deviation	E'' (GPa)	Standard deviation	E^* (GPa)
PP	1.59	0.12	0.11	0.01	1.59
PP-el	1.89	0.37	0.13	0.02	1.89
PVDF	3.12	0.41	0.16	0.03	3.12
PVDF-el	4.38	0.76	0.22	0.04	4.45
LDPE	1.02	0.42	0.18	0.07	1.04
LDPE-el	1.81	0.49	0.32	0.09	1.84

Table 4. Melting temperature and crystallinity values.

Compositions	T_{m1} (°C)	ΔH_{m1} (J/g)	Crystallinity ¹ (%)	T_{m2} (°C)	ΔH_{m2} (J/g)	Crystallinity ₂ (%)
PP	166.09	91.87	66.57	163.55	99.88	72.38
PP-el	165.82	104.35	75.62	163.47	101.68	73.68
PVDF	169.6	57.8	55.0	169.8	54.07	51.50
PVDF-el	169.4	66.6	63.5	169.46	53.83	51.27
LDPE	112.02	124.75	43.32	111.37	119.24	41.40
LDPE-el	112.04	151.67	52.66	111.93	119.06	41.34

₁ - measured properties for the first heating/cooling cycle; ₂ - measured properties for the second heating/cooling cycle.

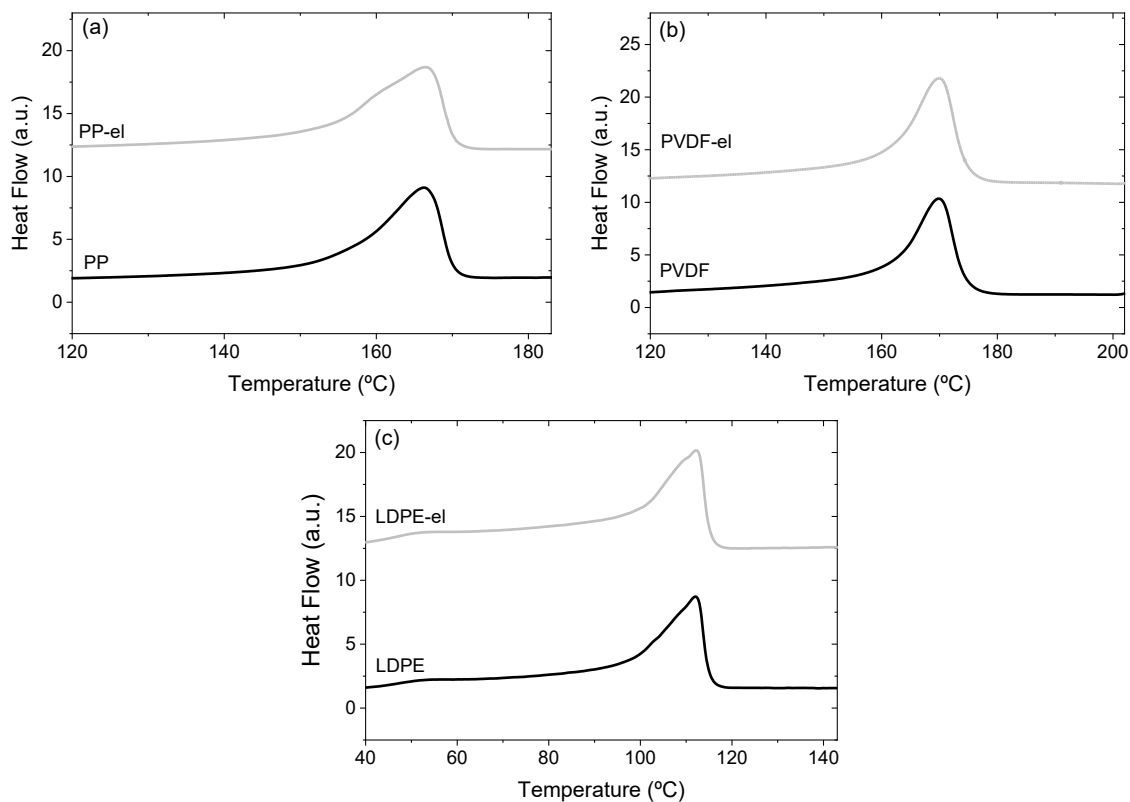


Figure 4. First Fusion peak for polymers processed with and without the extensional device for: (a) PP; (b) PVDF and (c) LDPE.

In this work, we demonstrated that it is possible to increase the crystallinity around 9%, for the polymers evaluated here, with the use of an extensional flow device coupled to a conventional extrusion process. This effect is probably associated with the FIC phenomenon, in which stress enhances the number of nuclei for crystals to grow, which in turn increases crystallinity. In addition, the use of controlled extension flows can also contribute to an increase in the mechanical properties as demonstrated by tensile tests and DMA, bringing an increase in Young's moduli (Figure 3) and in the maximum tensile strength (Table 2).

4. Conclusions

In brief, it was possible to produce filaments processed by extrusion with and without the extensional flow device. The association of the extensional flow in the processing of semi-crystalline polymers enhanced its crystallinity degree in 9.1%, 8.5% and 9.3%, respectively, for PP-el, PVDF-el, and LDPE-el, and this increase is probably related to FIC. The effects of the extensional flow both in the crystallinity and in the alignment of the chains also brought reflections on the mechanical properties. The storage moduli (E') increased by 18.9%, 40.4%, 77.5%, for PP-el, PVDF-el, and LDPE-el, respectively. This result was reaffirmed by the measurements made in the tensile test since the E' value is often related to the Young's moduli. The reflexes of this increase can be seen by the higher slopes for the samples

processed with the extensional flow device, indicating an increase in crystalline polymer stiffness.

The use of the elongational flow device increased the value of E'' by 18.2%, 37.5% and 77.8% for PP-el, PVDF-el, and LDPE-el, respectively. This effect can be associated with the morphological modification generated by the increase in the degree crystallinity and/or increased level of chain entanglement, that contribute to an increase in the degree of "internal friction" associated with the value of E'' .

5. Author's Contribution

- **Conceptualization** – Marcel Andrey de Goes; João Paulo Ferreira Santos; Benjamim de Melo Carvalho.
- **Data curation** – Marcel Andrey de Goes.
- **Formal analysis** – Marcel Andrey de Goes; João Paulo Ferreira Santos.
- **Investigation** – Marcel Andrey de Goes.
- **Methodology** – Marcel Andrey de Goes.
- **Project administration** – Benjamim de Melo Carvalho.
- **Resources** – Benjamim de Melo Carvalho.
- **Software** – Marcel Andrey de Goes.
- **Supervision** – NA.
- **Validation** – Marcel Andrey de Goes.
- **Visualization** – NA.

- **Writing – original draft** – Marcel Andrey de Goes.
- **Writing – review & editing** – Marcel Andrey de Goes; João Paulo Ferreira Santos.

6. Acknowledgements

The authors are grateful to Coordination for the Improvement of Higher Education Personnel (CAPES) and National Council for Scientific and Technological Development (CNPQ) for the financial support.

7. References

1. Keller, A., & Kolnaar, H. W. H. (2006). *Flow-induced orientation and structure formation*. In R. W. Cahn, P. Haasen & E. J. Kramer (Eds.), *Materials science and technology* (pp. 187-268). Germany: John Wiley & Sons, Ltda. <http://dx.doi.org/10.1002/9783527603978.mst0210>
2. Covas, J. A., Novais, R. M., & Paiva, M. C. (2011). *A comparative study of the dispersion of carbon nanofibres in polymer melts*. In *Proceedings of the 27th World Congress of the Polymer Processing Society* (pp. 1-5). Marocco: Polymer Processing Society. Retrieved in 2021, November 24, from https://repositorium.sdum.uminho.pt/bitstream/1822/14695/1/full_paper_dispersao_JAC_MCP.pdf
3. Vilaverde, C., Santos, R. M., Paiva, M. C., & Covas, J. A. (2015). Dispersion and re-agglomeration of graphite nanoplates in polypropylene melts under controlled flow conditions. *Composites. Part A, Applied Science and Manufacturing*, 78, 143-151. <http://dx.doi.org/10.1016/j.compositesa.2015.08.010>
4. Santos, R. M., Mould, S. T., Formánek, P., Paiva, M. C., & Covas, J. A. (2018). Effects of particle size and surface chemistry on the dispersion of graphite nanoplates in polypropylene composites. *Polymers*, 10(2), 222. <http://dx.doi.org/10.3390/polym10020222>. PMID:30966257.
5. Matsumoto, K., Nakade, Y., Sugimoto, K., & Tanaka, T. (2017). An investigation on dispersion state of graphene in polypropylene/graphite nanocomposite with extensional flow mixing. *AIP Conference Proceedings*, 1914(1), 150005. <http://dx.doi.org/10.1063/1.5016782>.
6. Carson, S. O., Maia, J. M., & Covas, J. A. (2016). A New extensional mixing element for improved dispersive mixing in twin-screw extrusion, Part 2: experimental validation for immiscible polymer blends. *Advances in Polymer Technology*, 37(1), 167-175. <http://dx.doi.org/10.1002/adv.21653>.
7. Chen, H., & Maia, J. M. (2021). Improving dispersive mixing in compatibilized polystyrene/polyamide-6 blends via extension-dominated reactive single-screw extrusion. *Journal of Polymer Engineering*, 41(5), 397-403. <http://dx.doi.org/10.1515/polyeng-2020-0230>.
8. Goes, M. A., Woicichowski, L. A., Rosa, R. V. V., Santos, J. P. F., & Carvalho, B. M. (2021). Improving the dispersion of MWCNT and MMT in PVDF melts employing controlled extensional flows. *Journal of Applied Polymer Science*, 138(17), 50274. <http://dx.doi.org/10.1002/app.50274>.
9. Mileva, D., Tranchida, D., & Gahleitner, M. (2018). Designing polymer crystallinity: an industrial perspective. *Polymer Crystallization*, 1(2), e10009. <http://dx.doi.org/10.1002/pcr2.10009>.
10. Maddah, H. A. (2016). Polypropylene as a promising plastic: a review. *American Journal of Political Science*, 6(1), 1-11. <http://dx.doi.org/10.5923/j.ajps.20160601.01>.
11. Santos, J. P. F., Arjmand, M., Melo, G. H. F., Chizari, K., Bretas, R. E. S., & Sundararaj, U. (2018). Electrical conductivity of electrospun nanofiber mats of polyamide 6/polyaniline coated with nitrogen-doped carbon nanotubes. *Materials & Design*, 141, 333-341. <http://dx.doi.org/10.1016/j.matdes.2017.12.052>.
12. Kumar Sen, S., & Raut, S. (2015). Microbial degradation of low density polyethylene (LDPE): a review. *Journal of Environmental Chemical Engineering*, 3(1), 462-473. <http://dx.doi.org/10.1016/j.jece.2015.01.003>.
13. Liu, Z. H., Pan, C. T., Lin, L. W., & Lai, H. W. (2013). Piezoelectric properties of PVDF/MWCNT nanofiber using near-field electrospinning. *Sensors and Actuators. A, Physical*, 193, 13-24. <http://dx.doi.org/10.1016/j.sna.2013.01.007>.
14. Chen, X., Xu, S., Yao, N., & Shi, Y. (2010). 1.6 v nanogenerator for mechanical energy harvesting using PZT nanofibers. *Nano Letters*, 10(6), 2133-2137. <http://dx.doi.org/10.1021/nl100812k>. PMID:20499906.
15. Boon, J., Challa, G., & Van Krevelen, D. W. (1968). Crystallization kinetics of isotactic polystyrene. I. Spherulitic growth rate. *Journal of Polymer Science. Part A-2, Polymer Physics*, 6(10), 1791-1801. <http://dx.doi.org/10.1002/pol.1968.160061009>.
16. Boon, J., Challa, G., & Van Krevelen, D. W. (1968). Crystallization kinetics of isotactic polystyrene. II. Influence of thermal history on number of nuclei. *Journal of Polymer Science. Part A-2, Polymer Physics*, 6(11), 1835-1851. <http://dx.doi.org/10.1002/pol.1968.160061102>.
17. Agar, A. W., Prank, F. C., & Keller, A. (1959). Crystallinity effects in the electron microscopy of polyethylene. *The Philosophical Magazine: A Journal of Theoretical Experimental and Applied Physics*, 4(37), 32-55. <http://dx.doi.org/10.1080/14786435908238226>.
18. Angelloz, C., Fulchiron, R., Douillard, A., Chabert, B., Fillit, R., Vautrin, A., & David, L. (2000). Crystallization of isotactic polypropylene under high pressure (γ phase). *Macromolecules*, 33(11), 4138-4145. <http://dx.doi.org/10.1021/ma991813e>.
19. Steiger, M. (2005). Crystal growth in porous materials - II: influence of crystal size on the crystallization pressure. *Journal of Crystal Growth*, 282(3-4), 470-481. <http://dx.doi.org/10.1016/j.jcrysgro.2005.05.008>.
20. Boyer, S. A. E., & Haudin, J.-M. (2010). Crystallization of polymers at constant and high cooling rates: A new hot-stage microscopy set-up. *Polymer Testing*, 29(4), 445-452. <http://dx.doi.org/10.1016/j.polymertesting.2010.02.003>.
21. Kong, W., Zhu, B., Su, F., Wang, Z., Shao, C., Wang, Y., Liu, C., & Shen, C. (2019). Melting temperature, concentration and cooling rate-dependent nucleating ability of a self-assembly aryl amide nucleator on poly(lactic acid) crystallization. *Polymer*, 168, 77-85. <http://dx.doi.org/10.1016/j.polymer.2019.02.019>.
22. Lagasse, R. R., & Maxwell, B. (1976). An experimental study of the kinetics of polymer crystallization during shear flow. *Polymer Engineering and Science*, 16(3), 189-199. <http://dx.doi.org/10.1002/pen.760160312>.
23. Amirdine, J., Htira, T., Lefevre, N., Fulchiron, R., Mathieu, N., Zinet, M., Sinturel, C., Burghélea, T., & Boyard, N. (2021). A novel approach to the study of extensional flow-induced crystallization. *Polymer Testing*, 96, 107060. <http://dx.doi.org/10.1016/j.polymertesting.2021.107060>.
24. Chellamuthu, M., Arora, D., Winter, H. H., & Rothstein, J. P. (2011). Extensional flow-induced crystallization of isotactic poly-1-butene using a filament stretching rheometer. *Journal of Rheology (New York, N.Y.)*, 55(4), 901-920. <http://dx.doi.org/10.1122/1.3593471>.
25. Haas, T. W., & Maxwell, B. (1969). Effects of shear stress on the crystallization of linear polyethylene and polybutene-1. *Polymer Engineering and Science*, 9(4), 225-241. <http://dx.doi.org/10.1002/pen.760090402>.
26. Bischoff White, E. E., Henning Winter, H., & Rothstein, J. P. (2012). Extensional-flow-induced crystallization of isotactic

- polypropylene. *Rheologica Acta*, 51(4), 303-314. <http://dx.doi.org/10.1007/s00397-011-0595-5>.
27. Harris, A. M., & Lee, E. C. (2008). Improving mechanical performance of injection molded PLA by controlling crystallinity. *Journal of Applied Polymer Science*, 107(4), 2246-2255. <http://dx.doi.org/10.1002/app.27261>.
 28. Feast, W. J., Tsibouklis, J., Pouwer, K. L., Groenendaal, L., & Meijer, E. W. (1996). Synthesis, processing and material properties of conjugated polymers. *Polymer*, 37(22), 5017-5047. [http://dx.doi.org/10.1016/0032-3861\(96\)00439-9](http://dx.doi.org/10.1016/0032-3861(96)00439-9).
 29. Jamali, S., Paiva, M. C., & Covas, J. A. (2013). Dispersion and re-agglomeration phenomena during melt mixing of polypropylene with multi-wall carbon nanotubes. *Polymer Testing*, 32(4), 701-707. <http://dx.doi.org/10.1016/j.polymertesting.2013.03.005>.
 30. Feigl, K., Tanner, F. X., Edwards, B. J., & Collier, J. R. (2003). A numerical study of the measurement of elongational viscosity of polymeric fluids in a semihyperbolically converging die. *Journal of Non-Newtonian Fluid Mechanics*, 115(2-3), 191-215. <http://dx.doi.org/10.1016/j.jnnfm.2003.08.002>.
 31. Líbano, E. V. D. G., Visconte, L. L. Y., & Pacheco, É. B. A. V. (2012). Thermal properties of polypropylene and organophilic bentonite. *Polímeros: Ciência e Tecnologia*, 22(5), 430-435. <http://dx.doi.org/10.1590/S0104-14282012005000063>.
 32. Peng, Q.-Y., Cong, P.-H., Liu, X.-J., Liu, T.-X., Huang, S., & Li, T.-S. (2009). The preparation of PVDF/clay nanocomposites and the investigation of their tribological properties. *Wear*, 266(7-8), 713-720. <http://dx.doi.org/10.1016/j.wear.2008.08.010>.
 33. Borhani zarandi, M., Bioki, H. A., Mirbagheri, Z.-a., Tabbakh, F., & Mirjalili, G. (2012). Effect of crystallinity and irradiation on thermal properties and specific heat capacity of LDPE & LDPE/EVA. *Applied Radiation and Isotopes*, 70(1), 1-5. <http://dx.doi.org/10.1016/j.apradiso.2011.09.001>.
 34. Münstedt, H. (2018). Extensional rheology and processing of polymeric materials. *International Polymer Processing*, 33(5), 594-618. <http://dx.doi.org/10.3139/217.3532>.
 35. Tabatabaei, S. H., Carreau, P. J., & Ajji, A. (2009). Effect of processing on the crystalline orientation, morphology, and mechanical properties of polypropylene cast films and microporous membrane formation. *Polymer*, 50(17), 4228-4240. <http://dx.doi.org/10.1016/j.polymer.2009.06.071>.
 36. Petrie, C. J. S. (2006). One hundred years of extensional flow. *Journal of Non-Newtonian Fluid Mechanics*, 137(1-3), 1-14. <http://dx.doi.org/10.1016/j.jnnfm.2006.01.010>.
 37. Pistor, V., Ornaghi, F. G., Ornaghi, H. L., & Zattera, A. J. (2012). Dynamic mechanical characterization of epoxy/epoxycyclohexyl-POSS nanocomposites. *Materials Science and Engineering A*, 532, 339-345. <http://dx.doi.org/10.1016/j.msea.2011.10.100>.
 38. Jawaid, M., Abdal Khalil, H. P. S., Hassan, A., Dungani, R., & Hadiyane, A. (2013). Effect of jute fibre loading on tensile and dynamic mechanical properties of oil palm epoxy composites. *Composites. Part B, Engineering*, 45(1), 619-624. <http://dx.doi.org/10.1016/j.compositesb.2012.04.068>.
 39. Saba, N., Jawaid, M., Alothman, O. Y., & Paridah, M. T. (2016). A review on dynamic mechanical properties of natural fibre reinforced polymer composites. *Construction & Building Materials*, 106, 149-159. <http://dx.doi.org/10.1016/j.conbuildmat.2015.12.075>.
 40. Das, A., & Satapathy, B. K. (2011). Structural, thermal, mechanical and dynamic mechanical properties of cenosphere filled polypropylene composites. *Materials & Design*, 32(3), 1477-1484. <http://dx.doi.org/10.1016/j.matdes.2010.08.041>.
 41. Correia, D. M., Costa, C. M., Lizundia, E., Sabater i Serra, R., Gómez-Tejedor, J. A., Biosca, L. T., Meseguer-Dueñas, J. M., Gomez Ribelles, J. L., & Lanceros-Méndez, S. (2019). Influence of Cation and anion type on the formation of the electroactive β -phase and thermal and dynamic mechanical properties of poly(vinylidene fluoride)/ionic liquids blends. *The Journal of Physical Chemistry C*, 123(45), 27917-27926. <http://dx.doi.org/10.1021/acs.jpcc.9b07986>.
 42. Sencadas, V., Lanceros-Méndez, S., Sabater i Serra, R., Andrio Balado, A., & Gómez Ribelles, J. L. (2012). Relaxation dynamics of poly(vinylidene fluoride) studied by dynamical mechanical measurements and dielectric spectroscopy. *The European Physical Journal. E, Soft Matter*, 35(5), 41. <http://dx.doi.org/10.1140/epje/i2012-12041-x>. PMID:22644136.
 43. Therese Pick, L., Harkin-Jones, E., Jovita Oliveira, M., & Clara Cramez, M. (2006). The effect of cooling rate on the impact performance and dynamic mechanical properties of rotationally molded metalocene catalyzed linear low density polyethylene. *Journal of Applied Polymer Science*, 101(3), 1963-1971. <http://dx.doi.org/10.1002/app.23709>.
 44. Joseph, K., Thomas, S., & Pavithran, C. (1993). Dynamic mechanical properties of short sisal fiber reinforced low density polyethylene composites. *Journal of Reinforced Plastics and Composites*, 12(2), 139-155. <http://dx.doi.org/10.1177/073168449301200202>.
 45. Majewsky, M., Bitter, H., Eiche, E., & Horn, H. (2016). Determination of microplastic polyethylene (PE) and polypropylene (PP) in environmental samples using thermal analysis (TGA-DSC). *The Science of the Total Environment*, 568, 507-511. <http://dx.doi.org/10.1016/j.scitotenv.2016.06.017>. PMID:27333470.
 46. Sližová, M., Stašek, M., & Raab, M. (2020). Polypropylene after thirty years of storage: mechanical proof of heterogeneous aging. *Polymer Journal*, 52(7), 775-781. <http://dx.doi.org/10.1038/s41428-020-0327-8>.
 47. Santos, J. P. F., da Silva, A. B., Arjmand, M., Sundararaj, U., & Bretas, R. E. S. (2018). Nanofibers of poly(vinylidene fluoride)/copper nanowire: microstructural analysis and dielectric behavior. *European Polymer Journal*, 101, 46-55. <http://dx.doi.org/10.1016/j.eurpolymj.2018.02.017>.
 48. Li, D., Zhou, L., Wang, X., He, L., & Yang, X. (2019). Effect of crystallinity of polyethylene with different densities on breakdown strength and conductance property. *Materials (Basel)*, 12(11), 1746. <http://dx.doi.org/10.3390/ma12111746>. PMID:31146397.
 49. Wu, W., & Wang, Y. (2020). Physical and thermal properties of high-density polyethylene film modified with polypropylene and linear low-density polyethylene. *Journal of Macromolecular Science, Part B: Physics*, 59(4), 213-222. <http://dx.doi.org/10.1080/00222348.2019.1709710>.
 50. Dusunceli, N., & Colak, O. U. (2008). Modelling effects of degree of crystallinity on mechanical behavior of semicrystalline polymers. *International Journal of Plasticity*, 24(7), 1224-1242. <http://dx.doi.org/10.1016/j.ijplas.2007.09.003>.

Received: Nov. 24, 2021

Revised: June 23, 2022

Accepted: July 01, 2022